NONLINEAR OPTICAL PHENOMENA DOI: 10.1070/QEL15979

Optical parametric oscillator of mid-IR, visible and UV ranges with synchronous pumping by a *Q*-switched mode-locked Nd:YAG laser

V.I. Donin, M.D. Yakovin, D.V. Yakovin

Abstract. **The parametric generation in a nonlinear PPLN crystal synchronously pumped by a *Q*-switched mode-locked Nd:YAG laser with a pulse duration of 45 ps is studied. The output pump intensity in the nonlinear crystal reaches ~10 GW cm^{-2}. At a pulse repetition rate of 1 kHz, the average output power at the idler wavelength (~3.6 μm) is ~12 mW, the peak power is ~25 kW, and the conversion efficiency (with respect to the absorbed power) is ~10%. The radiation linewidth at the signal wavelength (~1.5 μm) is 13 cm^{-1}. Along with the signal and idler waves, the output emission spectrum contains lines at wavelengths of 822, 754, 624, 532, 463, 442, 392 and 355 nm. The tunable radiation with wavelengths in the vicinity of 392, 463 and 822 nm is observed for the first time. The tuning ranges for the new lines are measured (5–10 nm) and their origin is explained.**

Keywords: *parametric generation, Nd:YAG laser, synchronous pumping, Q switching, mode locking.*

1. Introduction

The development of new methods for implementing optical parametric generation in the mid-IR range remains an urgent problem. The interest of researchers to mid-IR optical parametric oscillators (OPOs) is related not only to their practical applications in various fields (medicine, safety systems, sensing atmosphere, etc.), but also to the necessity of increasing the sensitivity of the methods developed previously on the basis of laser absorption spectroscopy (photoacoustic spectroscopy, CRD spectroscopy, etc.). The studies aimed at developing high-power tunable OPOs with quasi-phase-matched type of phase interaction on periodically poled lithium niobate (PPLN) crystals are of particular interest due to their large nonlinear coefficients, high efficiency, relatively high damage thresholds, availability and acceptable prices. For example, average output powers of 22.6 and 63 W at wavelengths of 3.8 and 1.47 2 μm, respectively, were obtained when pumping a PPLN crystal by a nanosecond *Q*-switched Nd:YAG laser [1]. The average pump power was 150 W, the pulse repetition rate was 10 kHz and the pump pulse duration was 120 ns. A parametric frequency conversion in a PPLN crystal pumped by nano-, pico- and femtosecond pulses was implemented in [2]. The conversion efficiency of a picosecond OPO was 14% and 12% at idler wavelengths of 3.5 and 4.5 μm, respectively.

In this paper, we report the results of studying the parametric generation in a nonlinear element with quasi-phase-matched type of interaction under synchronous pumping by a 45-ps pulsed Nd:YAG laser. A doped MgO (5 mol%) PPLN crystal (*Z*-cut) with sizes of 5×1×20 mm and two 'tracks', having periods of a regular domain structure of 29.5 and 30 μm, was used as a nonlinear element. The singly resonant OPO scheme was applied, and pumping was performed by a *Q*-switched mode-locked Nd:YAG laser using a spherical mirror and acousto-optic modulator (the SMAOM method [3]).

The pump laser, along with the implementation of the mode-locking regime and *Q*-factor modulation using a traveling-wave modulator, had another specific feature: a detuning of the cavity length from the value $L_0 = c/(4f) \approx 1.5$ m (where c is the speed of light and f is the sound wave frequency in the modulator) by displacing the output cavity mirror led to a splitting of some picosecond pulses into two or more pulses (depending on the detuning value). This effect is related to the excitation of several competing transverse modes, which led to non-single-shot generation under mode-locking conditions with a time interval of ~100 ps between the pulses [4].

2. Experimental setup

Figure 1 shows a schematic of the experimental setup with a singly resonant OPO, which was used in our study. A 1064.5-nm pump laser PL, implemented according to the scheme [4], emitted a train of pulses with a repetition rate of 1 kHz, train

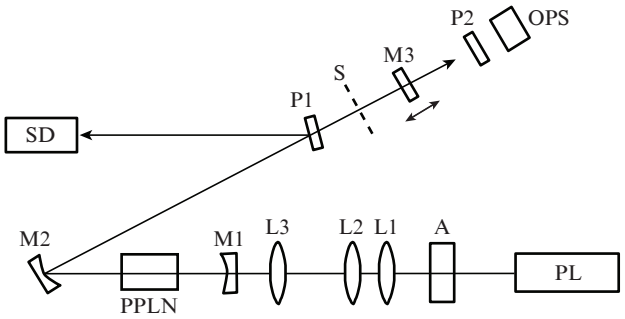

Figure 1. Schematic of the experimental setup: (PL) Nd:YAG pump laser; (SD) spectral device; (OPS) optical power sensor; (A) polarisation attenuator; (L1, L2) matching lenses; (L3) focusing lens; (PPLN) nonlinear crystal; (M1, M2, M3) OPO cavity mirrors; (P1) sapphire plate; (P2) germanium plate; (S) absorbing screen.

V.I. Donin, M.D. Yakovin, D.V. Yakovin Institute of Automation and Electrometry, Siberian Branch, Russian Academy of Sciences, prosp. Akad. Koptyuga 1, 630090 Novosibirsk, Russia; e-mail: donin@iae.nsk.su, m.d.yakovin@mail.ru

Received 27 November 2015; revision received 4 March 2016
Kvantovaya Elektronika **46** (7) 601–605 (2016)
Translated by Yu.P. Sin'kov

duration of ~100 ns and an individual pulse duration of 45 ps in the train. The peak power was ~1 MW. The pump power incident on the PPLN crystal was gradually controlled using a polarisation attenuator A.

The OPO cavity was formed by mirrors M1, M2 and M3. Mirror M1 (Layertec, Germany) had a radius of curvature of 100 mm, a reflectance $R_{1.4-1.7}$ = 99.5% in the range of 1.4–1.7 μm, and a transmittance of about 99% at a wavelength of 1.06 μm. Copper mirror M2 had a radius of curvature of 125 mm and reflectances $R_{1.0-1.7}$ = 90% and $R_{3.0-4.0}$ = 97%. Flat output mirror M3 on a ZnSe substrate (Layertec) ($R_{1.2-1.7}$ = 99.5%) had a high transmittance at 1.06 μm (78%) and in the range of 3.0–4.0 μm (99.5%). This mirror could be displaced along the cavity axis using an adjusting device. A sapphire plate P1 was oriented at an angle close to the angle of normal incidence with respect to the cavity axis and reflected about 15% radiation intensity from the cavity into the spectral device SD or on the power meter. Germanium plate P2 was used to select idler wavelengths. Lenses L1 and L2 were used to reduce the PL beam divergence. Lens L3 (with a focal length of 250 mm) focused the pump beam into the PPLN crystal. The pump beam diameter in the waist was 160 μm.

A screen S was applied to observe the superluminescence regime, where the cavity was absent and generation occurred during one pass through the nonlinear crystal. The crystal was placed in a thermostat, the temperature of which was controlled with a PID controller. The spectral device was either an STS-VIS scanning spectrometer or an MDR-23 monochromator (the monochromator input and output slits were 50 μm wide, and the inverse linear dispersion was 1.2 nm mm^{-1}) with an FEU-68 photomultiplier. The power at the idler wavelength was monitored and measured with a pyroelectric photodetector or an optical power sensor (OPS) of Thorlabs s302c type.

3. Experimental results

The OPO was tuned by changing the crystal temperature from 20 to 150 °C. The dependence of the OPO output power on the detuning of the pump laser cavity length, ΔL_p, measured at a double excess above the OPO generation threshold, is presented in Fig. 2. Here, $\Delta L_p = 0$ corresponds to the single-shot regime of the Nd : YAG laser, at which the contributions of the single and double picosecond pulses to the total laser intensity were more than 95% and ~5%, respectively. Since undesirable effects ('gray tracks', surface and volume damage) were observed in the crystal in the single-shot regime, where the peak pump intensity reached 10 GW cm^{-2}, further measurements were performed at detunings of the output pump laser mirror ΔL_p = 300 μm (in this case, the pump laser generated ~53% single, 37% double and ~10% triple pulses) and 700 μm (25% single, 45% double, 20% triple and 10% quadruple pulses).

Figure 3 shows the dependences of the signal-wave power in the OPO cavity [P_{sign}, curve (*1*)] and the output idler-wave power [P_{idle}, curve (*2*)] on the average pump power P_p for the configuration with a sapphire plate and the dependence of the output idler-wave power [curve (*3*)] without this plate at room temperature (~25°C) of the PPLN crystal on the track with a period of 30 μm. The threshold pump power was ~100 mW in the entire specified range of crystal temperatures and changed only slightly with variation in temperature.

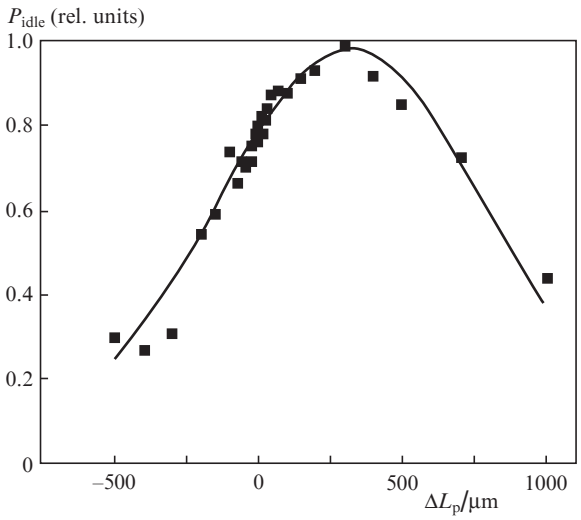

Figure 2. Dependence of the output power P_{idle} at the idler wavelength on the detuning ΔL_p of the output mirror of the pump laser cavity.

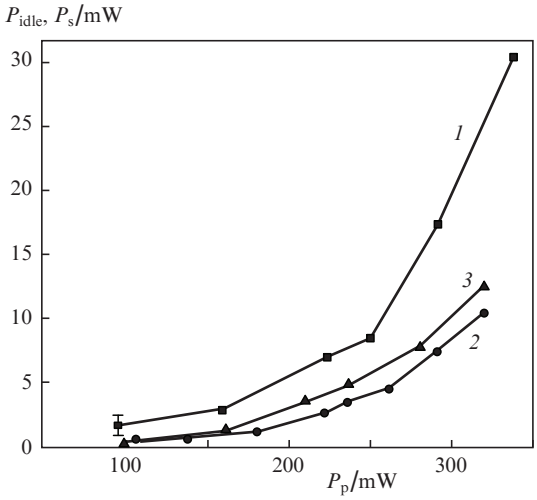

Figure 3. Dependences of the idler-wave output power P_{idle} and signal-wave power P_s in the cavity on the average pump power at ΔL_p = 300 μm: (*1*, *2*) the signal-wave power in the OPO cavity and the idler-wave output power with plate P1, respectively, and (*3*) the idler-wave output power without a plate.

The signal-wave radiation was extracted from the cavity using a sapphire plate (the total reflection loss from the plate faces was ~30%). Part of radiation was recorded by a power meter equipped with a light filter having a transparency window in the range of 1.4–1.6 μm to estimate the power in the cavity. To increase the pump–idler wave conversion efficiency, plate P1 was removed from the cavity. In this case, the average output power at the idler wavelength reached 12 mW.

We also measured the pump power P_{out} transmitted through the OPO (with allowance for the transmittance of mirror M3) as a function of the incident radiation power P_p, and the data obtained were used to calculate the pump absorption coefficient $k = 1 - \alpha - P_{out}/P_{in}$; here, α is the loss on mirrors in the OPO cavity, which turned out to be 10% (generally on the mirror with a copper coating). The pump absorption coefficient was ~50%. Thus, the conversion efficiency for the idler wave with respect to the absorbed power was ~10%. Note that the pump absorption and output power

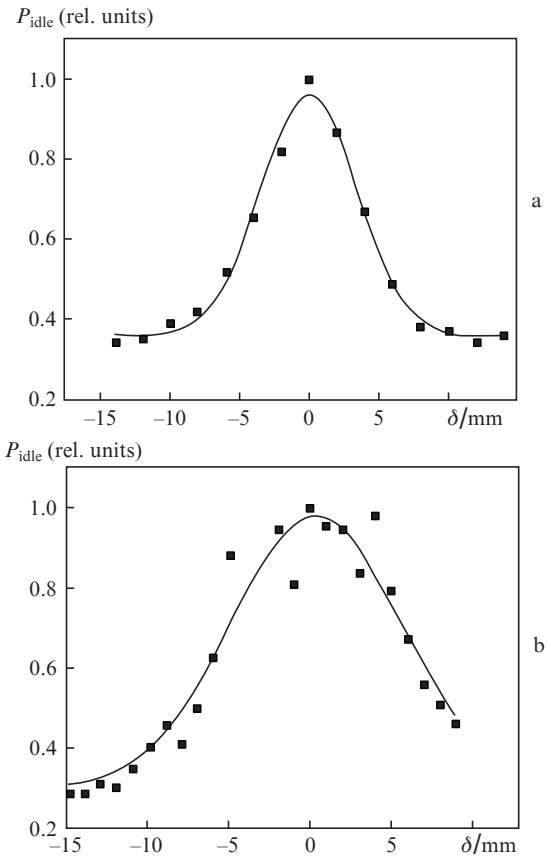

Figure 4. Dependences of the relative idler-wave output power P_{idle} on the change in the OPO cavity length δ at pump-laser cavity detunings of (a) 300 and (b) 700 μm.

could be increased by increasing the length of nonlinear PPLN crystal.

A necessary condition for implementing efficient generation of parametric radiation is to provide matching between the intermodal frequency of the OPO cavity and the intermodal frequency of the pump laser, which was done by choosing the same cavity lengths for the pump laser ($L_0 \approx 1.5$ m) and OPO. Their exact matching was obtained by displacing mirror M3 along the OPO cavity axis. Figure 4 shows a dependence of the output power on the change in the OPO cavity length δ at different detunings ΔL_p. It can be seen that an increase in ΔL_p from 300 to 700 μm leads to an increase in the curve FWHM from 8 to 10 mm.

The tuning temperature characteristic for the signal wavelength was measured on two tracks of the PPLN crystal with periods of 30 and 29.5 μm. The tuning characteristic for the idler wavelength was calculated based on these data. The thus found tuning characteristics in the ranges of 1.48–1.55 and 3.4–3.8 μm are shown in Fig. 5. A change in the crystal temperature by $\Delta T = 130$ °C results in detuning of the idler and signal wavelengths by ~400 and ~70 nm, respectively. The generation linewidth at the signal wavelength, measured at

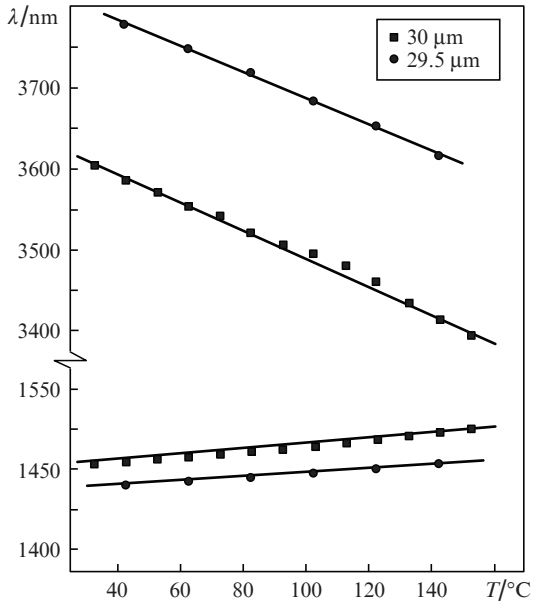

Figure 5. Tuning characteristic of the PPLN crystal on two tracks with periods of 29.5 and 30 μm.

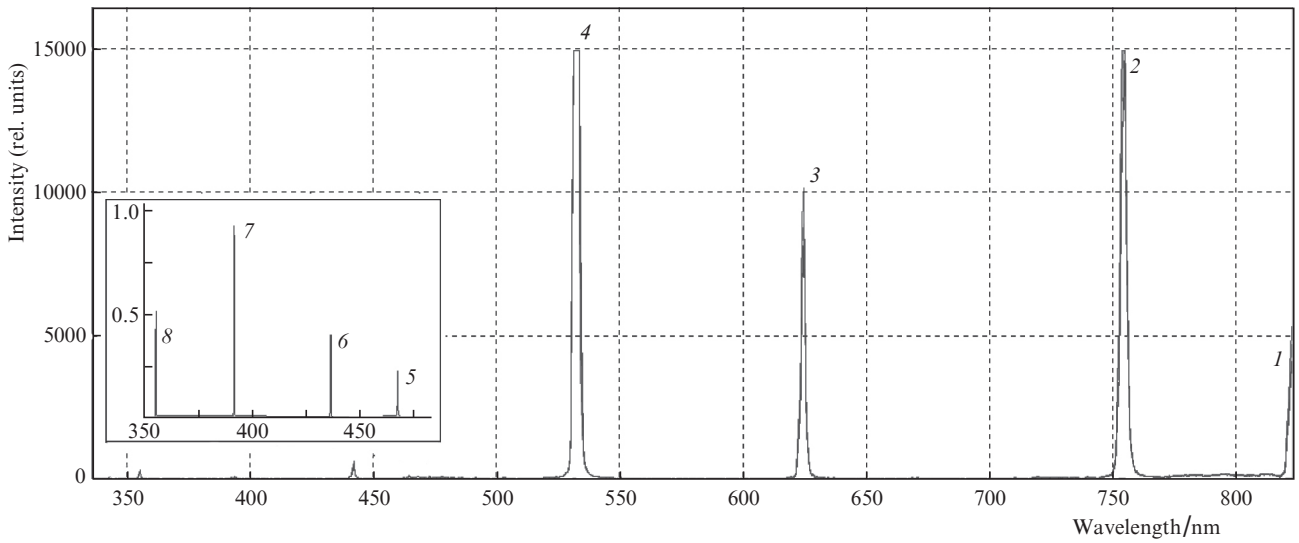

Figure 6. Panoramic spectrum of output radiation in the range of 350–830 nm, with lines at (*1*) 822, (*2*) 754, (*3*) 624, (*4*) 532, (*5*) 463, (*6*) 442, (*7*) 392 and (*8*) 354.7 nm. The inset shows the lines recorded with an MDR-23 monochromator.

room temperature on a track with a period of 30 μm, was found to be 13 cm^{-1} (or 390 GHz).

Parametric generation occurred also in the superluminescence regime, where an opaque screen was installed before output mirror M3. In both cases, along with the idler and signal waves, the output emission spectrum contained lines in the visible range. However, the lines were much stronger in the parametric generation regime.

All measurements in the visible range were performed in the stable-cavity regime (i.e., there was no screen before mirror M3) on a track with a 30-μm period. A spectrogram recorded in the range of 350–830 nm at room crystal temperature is presented in Fig. 6. Along with the second-harmonic generation lines from the pump (532 nm) and signal (754 nm) waves, the spectrum contained spectral lines with centre wavelengths of 624, 463, 442, 392 and 354.7 nm. Lines (*1–4*) in Fig. 6 are wider because of the lower resolution (~2 nm) of the panoramic spectrometer. We should also note that a PS-15 light filter was placed at the input of the STS-VIS spectrometer, which reduced the intensities of lines at 532 and 624 nm by factors of 40 and 30, respectively.

The linewidths measured with an MDR-23 monochromator we equal to $\Delta\nu_{355} \approx 250$ GHz, $\Delta\nu_{392} \approx 360$ GHz, $\Delta\nu_{442} \approx 350$ GHz, $\Delta\nu_{463} \approx 230$ GHz, $\Delta\nu_{532} \approx 200$ GHz, $\Delta\nu_{624} \approx 400$ GHz and $\Delta\nu_{822} \approx 230$ GHz.

The conversion efficiency (with respect to the absorbed pump power) for the emission lines at 619, 532, 436 and 392 nm was measured with a change in the crystal temperature. In this case, a diffraction grating and an Ophir Vega power meter (PD300) played the role of a spectral device.

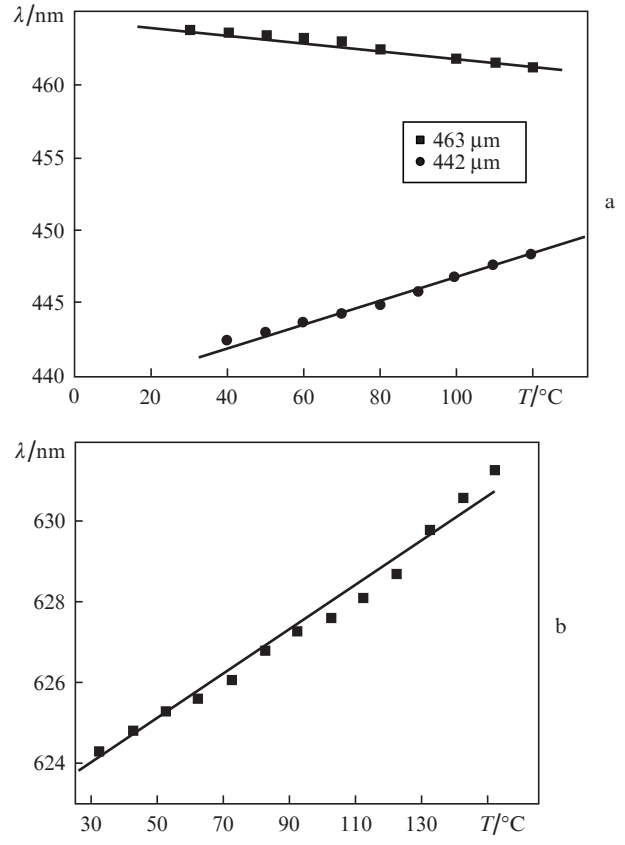

Figure 7. Tuning characteristics of the PPLN crystal at wavelengths of (a) 442 and 463 nm and (b) 624 nm.

Table 1.

T (°C)	η_{624} (%)	η_{532} (%)	η_{442} (%)	η_{392} (%)
137	0.09	0.12	0.06	0.13
97	0.06	0.19	0.04	0.09
23.5	0.05	0.05	0.04	0.08

Table 1 contains the values of the conversion efficiency η obtained at different temperatures.

The change in the wavelengths of visible-range lines with a change in the nonlinear-crystal temperature is shown in Fig. 7.

4. Analysis of the results

The main specific feature of the quasi-phase-matched interaction is that the energy transfer from the pump wave to the idler and signal waves should in principle occur efficiently throughout the entire length of the nonlinear crystal. According to [5], at a threefold excess of the pump intensity above the threshold, in the case of Gaussian beams, the pump depletion is 50%; this value is in agreement with our experimental data. The one-pass gain in the high-intensity approximation, in the case of Gaussian beams and under optimal focusing conditions, is given by the formula [6, 7]

$$G \approx \frac{1}{4}e^{2\Gamma},$$

where the specific gain

$$\Gamma = 2\pi d_{\text{eff}} \sqrt{\frac{2 g_s g_t I_p k}{n_s n_i n_p \varepsilon_0 c \lambda_s \lambda_i}};$$

$n_{s,i,p}$ are the refractive indices of the PPLN crystal at the signal, idler and pump wavelengths, respectively; d_{eff} is the effective nonlinear coefficient of PPLN crystal; $l = 20$ mm is the length of PPLN crystal; $\lambda_{p,s,i}$ are the pump, signal and idler wavelengths, respectively; c is the speed of light; ε_0 is the permittivity; I_p is the pump power density in the crystal waist (the waist radius is w_p); $g_s = w_p^2/(w_s^2 + w_p^2)$ and $g_t = \sqrt{\tau_p^2/(\tau_s^2 + \tau_p^2)}$ (in our case, $g_s = 0.9$ and $g_t = 0.86$); $k = 0.5$ is the pump depletion coefficient; and τ_p and τ_s are the pump and signal pulse durations, respectively. At $I_p \approx 2$ GW cm^{-2} (which corresponds to $\Delta L_p = 300$ μm and $w_p \approx 80$ μm), $d_{\text{eff}} = 14$ pm V^{-1} and $\lambda_s = 1.51$ μm; the gain is $G \approx 3 \times 10^{12}$.

With allowance for the fact that the average output power $P_{\text{idle}} = 12$ mW and that the emission pulse at the idler and signal wavelengths is shortened (according to [8]) to ~30 ps, the output peak power is

$$P_m = \frac{P_{\text{idle}}}{NF\tau_i} 0.64 \approx 25 \text{ kW},$$

where N is the number of picosecond pulses in the train at its half maximum; F is the repetition rate of train pulses; and the factor 0.64 is a correction to the non-single-shot character of generation.

Let us consider the data of Fig. 4. Under the conditions of synchronous OPO pumping (see, e.g., [9]), cavity detuning width δ is generally $(1/20–1/10)c\tau_p$. The detuning width for a synchronously pumped OPO cavity is also governed, along with τ_p, by the group-velocity dispersion for the pump and signal-wave pulses. The δ value was increased to $\sim 0.25c\tau_p$ in [10] by compensating for the cavity dispersion using a diffrac-

tion grating. In our case, $\delta \sim c\tau_p$ without using any elements for dispersion compensation, and this result is somewhat unusual. The enlarged width of the curves in Fig. 4 is a consequence of the short time interval between the pulses (in comparison with the time of double cavity round trip in the non-single-shot regime). One might expect the OPO cavity detuning not to affect the generation power at high repetition rates of pump pulses (above 10 GHz).

The spectral lines observed in the near-UV and visible ranges are the result of mixing of the pump-wave (ω_p) and signal-wave (ω_s) frequencies, which occurs in a nonlinear crystal:

$$2\omega_p = \omega_{532},\ 2\omega_s = \omega_{754},\ \omega_p + \omega_s = \omega_{624},\ 3\omega_p - \omega_s = \omega_{463},$$

$$\omega_p + 2\omega_s = \omega_{442},\ 2\omega_p + \omega_s = \omega_{392},\ 3\omega_p = \omega_{355},\ 2\omega_p - \omega_s = \omega_{822}.$$

With a change in the crystal temperature, the lines generated with participation of the signal wave were shifted due to the signal-wave detuning (Fig. 7). The lines at 624 and 442 nm were observed previously [11, 12], whereas the tunable lines at 392, 463 and 822 nm were observed for the first time.

As was indicated above, the conversion efficiency at the idler wavelength was found to be ~10%. It decreases due to the processes of frequency mixing and second- and third-harmonic generation. This efficiency can be reduced due to the generation of not only recorded but also some other lines, e.g., the line $3\omega_p + \omega_s = \omega_{286}$, which is absorbed by the nonlinear crystal.

The conversion efficiency of tunable lines in the visible and UV ranges can be increased by fabricating a PPLN crystal in the form of two or three sections, each having an individual period. In this way, a conversion efficiency of 21% was obtained on the 624-nm line in the continuous regime in [11].

Thus, the main features of an OPO based on a PPLN crystal, synchronously pumped by a *Q*-switched mode-locked Nd:YAG laser using the SMAOM method, were investigated. In particular, it was found that the use of this method allows one to significantly reduce the requirements to the accuracy of matching the cavity lengths for the pump laser and OPO. Along with the signal (1.48–1.55 μm) and idler (3.4–3.8 μm) wavelengths, the output spectrum contained lines at 822, 754, 624, 532, 463, 442, 392 and 355 nm. The tunable lines at 392, 463 and 822 nm were observed for the first time. The tuning ranges of the new lines were measured (5–10 nm), and their origin was explained.

Acknowledgements. We are grateful to D.B. Kolker for kindly supplying a mirror on a ZnSe substrate and for the useful discussion.

References

1. Peng Y., Wei X., Wang W., Li D. *Opt. Commun.*, **283**, 4032 (2010).
2. Anstett G., Ruebel F., L'huillier J.A. *Proc. SPIE Int. Soc. Opt. Eng.*, **7483**, 74830A (2009).
3. Donin V.I., Yakovin D.V., Gribanov A.V. *Opt. Lett.*, **37**, 338 (2012).
4. Donin V.I., Yakovin D.V., Gribanov A.V. *Kvantovaya Elektron.*, **45**, 1117 (2015) [*Quantum Electron.*, **45**, 1117 (2015)]
5. Bjorkholm J.E. *IEEE J. Quantum Electron.*, **7**, 109 (1971).
6. Harris S.E. *Proc. IEEE*, **57**, 2096 (1969).
7. McCarthy M.J., Hanna D.C. *J. Opt. Soc. Am. B*, **10**, 2180 (1993).
8. Becker M.F., Kuizenga D.J., Phillion D.W., et al. *J. Appl. Phys.*, **45**, 3996 (1974)
9. Graf T., McConnell G., Fergusson A., et al. *Appl. Opt.*, **38**, 3324 (1999).
10. Laporte C., Dherbecourt J., Melkonian J., et al. *J. Opt. Soc. Am. B*, **31**, 1026 (2014).
11. Bosenberg W.R., Alexander J.I., Myers L.E., et al. *Opt. Lett.*, **23**, 207 (1998)
12. Abu-Safe H.H. *Appl. Opt.*, **44**, 7458 (2005).